Thin Solid Films 546 (2013) 236–241

Contents lists available at ScienceDirect

Thin Solid Films

journal homepage: www.elsevier.com/locate/tsf

Preparation and characterization of highly transparent epoxy/inorganic nanoparticle hybrid thin films

Yang-Yen Yu [a,b,c,*], Yu-Cyuan Rao [a], Chao-Ching Chang [d]

[a] Department of Materials Engineering, Ming Chi University of Technology, 84 Gungjuan Rd., Taishan Dist., New Taipei City 24301, Taiwan
[b] Center for Thin Film Technologies and Applications, Ming Chi University of Technology, 84 Gungjuan Rd., Taishan Dist., New Taipei City 24301, Taiwan
[c] Battery Research Center of Green Energy, Ming Chi University of Technology, 84 Gungjuan Rd., Taishan Dist., New Taipei City 24301, Taiwan
[d] Department of Chemical and Materials Engineering, Tamkang University, 151 Yingzhuan Rd., Tamsui Dist., New Taipei City 25137, Taiwan

ARTICLE INFO

Available online 17 May 2013

Keywords:
Epoxy-titania hybrid materials
High transparent films
Thermal polymerization
Refractive index
Sol–gel method

ABSTRACT

This paper presents the preparation of epoxy/inorganic-nanoparticle hybrid materials synthesized from diglycidyl ether of bisphenol A and colloidal titania (TiO_2) with coupling agent, 3-isocyanatopropyltriethoxysilane, and curing agent, hexahydro-4-methylphthalic anhydride, by using a thermal polymerization. The precursor was spin-coated and thermal-cured to form hybrid films. The experimental results showed that the refractive index of hybrid films can be tuned by adding various solid contents of TiO_2 to hybrid films. The refractive index at 633 nm increased from 1.450 to 1.639 as the TiO_2 content increased from 0 to 50 wt.%. UV–vis analysis showed that the transparency of hybrid films was over 90%. L.a.b. color analysis indicated that the luminance of films was above 95%, and no yellowing was observed. In addition, the hybrid materials exhibited a low hydroscopic property under a high-humidity environment.

1. Introduction

Organic/inorganic hybrid materials have recently been studied extensively. Organic materials have been widely used because of their flexibility, toughness, and processability. Although inorganic materials have high heat resistance [1], they have excellent mechanical and optical properties [2–5]. Organic/inorganic hybrid materials have a combination of the superior properties of both organic polymers and inorganic materials. The properties of hybrid materials can be tuned through the functionality or segment size of each component. Mixing hybrid materials in the molecular level using Vander Waals forces, hydrogen bonding, and ionic or covalent bonding [6] can overcome the traditional composite macroscopic phase separation to ensure excellent characteristics of organic and inorganic substances [7–11]. The properties (optical, mechanical, and thermal) of hybrid materials are relative to those of each component, the composite phase morphology, and interfacial properties. The mild characteristics offered using the sol–gel process allow inorganic and organic components to be mixed at the nanometric scale [12,13].

Epoxy resin systems are commonly used as matrices in composite materials for a wide range of automotive and aerospace applications, shipbuilding, and electronic devices. Highly cross-linked epoxy matrices can provide high stiffness and strength; however, they are often brittle because plastic deformation is constrained [14,15]. To develop technical nanocomposites, several researchers applied inorganic nanoparticles to improve various properties. Bauer et al. [16] showed that a high content of nanosized silica, alumina, and titania was embedded in epoxy adhesives. The reinforced nanocomposites exhibited shifts of glass transition temperatures of approximately 20 K, indicating improved thermal stability. Chau et al. [17] prepared epoxy/titania (TiO_2) nanocomposite coatings with a high refractive index and optical transparency by using the sol–gel method. Nanocomposite coating with a refractive index of 1.668 can be obtained by adding 30 wt.% TiO_2 nanoparticles into the polymer matrix. Coatings with various amounts of TiO_2 exhibited excellent optical transparency of more than 90%. Although a nanocomposite with a higher refractive index can be obtained by increasing the TiO_2 content, cracks appear on the surface of the hybrid coating. They also showed that the refractive index of hybrid films can be tuned using various forms of titania nanoparticles and by changing the solid content of titania. The solid content of titania in the epoxy matrix can be more than 70 wt.% without affecting the optical transparency of the hybrid film [18]. Sowntharya et al. [19] synthesized hybrid nanocomposite coatings from titanium tetraisopropoxide, and epoxy or acrylic modified silanes were deposited on polycarbonate (PC). The results showed that the coatings from a freshly prepared sol of acrylic modified silane and titania exhibited a maximal nanoindentation hardness of 0.52 GPa compared to 0.23 GPa for bare PC.

We prepared epoxy/TiO_2 hybrid films using the colloidal titania and diglycidyl ether of bisphenol A (DGEBA) with a 3-isocyanatopropyltriethoxysilane (IPTES) coupling agent and hexahydro-

* Corresponding author at: Department of Materials Engineering, Ming Chi University of Technology, 84 Gungjuan Rd., Taishan Dist., New Taipei City 24301, Taiwan. Tel.: +886 2 29089899 4676; fax: +886 2 29084091.
E-mail address: yyyu@mail.mcut.edu.tw (Y.-Y. Yu).

0040-6090/$ – see front matter © 2013 Elsevier B.V. All rights reserved.
http://dx.doi.org/10.1016/j.tsf.2013.05.038

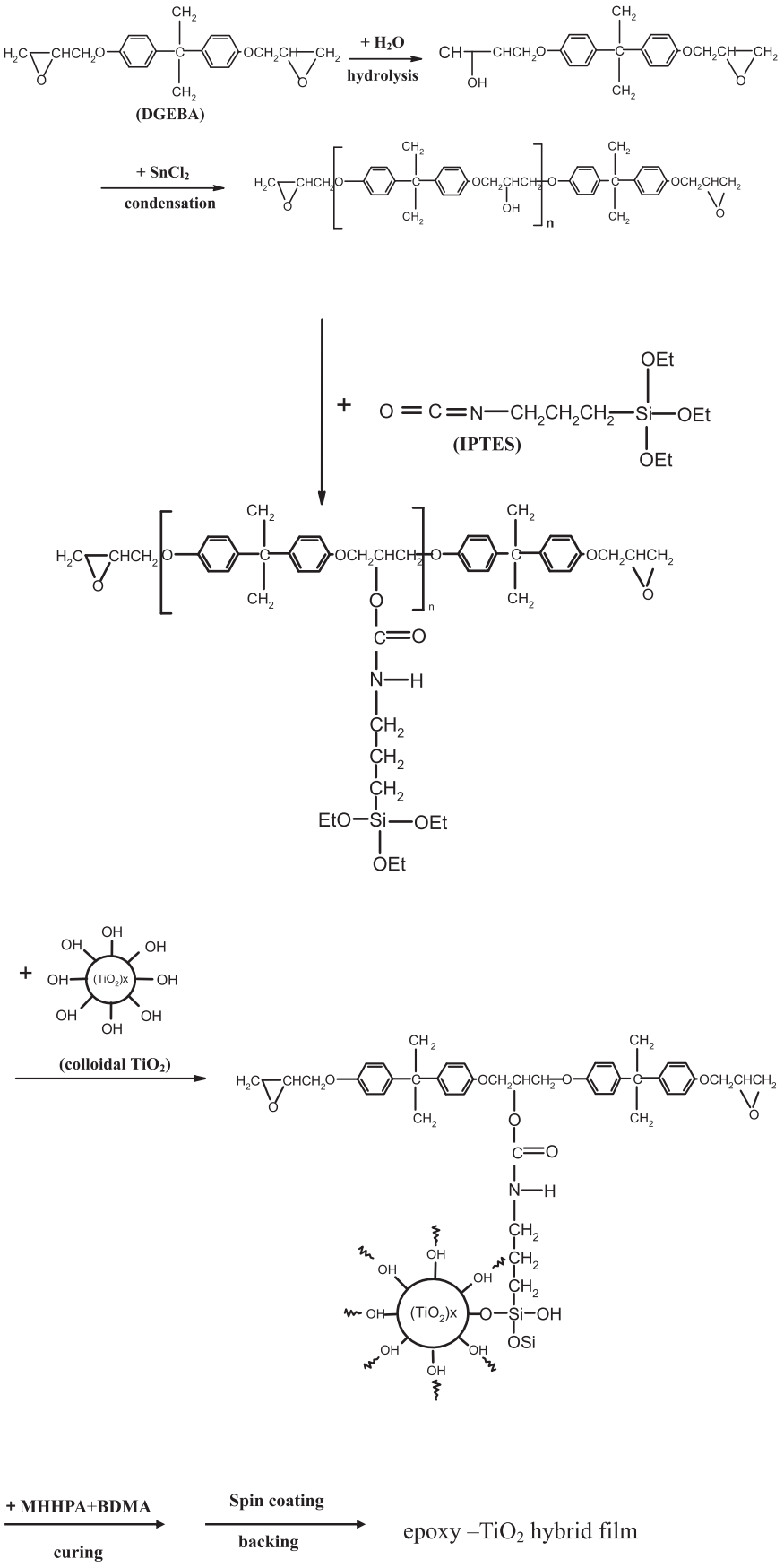

Fig. 1. Reaction scheme for preparing epoxy/TiO_2 hybrid films.

4-methylphthalic anhydride (MHHPA) curing agent by using a thermal polymerization. The precursor was spin-coated and thermal-cured to form hybrid films. DGEBA is widely used in adhesive, electronic, wear resistance, and light-emitting diode packaging because of the small volume of shrinkage during curing. The reaction scheme for preparing epoxy/TiO_2 hybrid films is shown in Fig. 1. The effects of the solid content of titania on the optical and thermal properties of epoxy/TiO_2 hybrid films were also examined.

2. Experimental details

2.1. Materials

Titanium n-butoxide monomer ($Ti(OBu)_4$, 99%, TCI), n-butanol (BuOH, 99%, ECHO), hydrochloric acid (HCl, > 35%, TOKYO), bisphenol A diglycidyl ether resin (DGEBA, 99%, TCI), 3-isocyanatopropyltriethoxysilane (IPTES, 95%, Alfa Aesar), hexahydro-4-methylphthalic anhydride (MHHPA, 96%, Aldrich), n,n-dimethylbenzylamin (BDMA, 98%, Alfa Aesar) as a promoter, Tin(II) chloride(98%, MERCK) as a catalyst, and butanone (95%, TEDIA) were used as solvent for the synthesis of epoxy/TiO_2 hybrid materials.

2.2. Preparation of colloidal TiO_2

The typical procedure for the preparation of colloidal TiO_2 is as follows. First, Solution A was prepared by adding $Ti(OBu)_4$ in BuOH and stirring for 30 min. Subsequently, Solution B was prepared by adding the desired amount of HCl and de-ionized water in butanol and stirring for 30 min. Moreover, Solution B was slowly dropped into Solution A and stirred for 2 h to obtain the colloidal TiO_2 solution.

2.3. Preparation of epoxy/TiO_2 hybrid materials

DGEBA and IPTES were dissolved in butanone and poured into a three-neck round-bottom flask and stirred under a nitrogen flow for 3 h. The previously obtained colloidal TiO_2 was subsequently added into the flask to form a yellowish solution. It was noticed that the colloidal TiO_2 should be added by consecutive dropwise addition for preventing the aggregation between the TiO_2 nanoparticles. Subsequently, the MHHPA and BDMA were mixed into the flask and stirred under a nitrogen flow for 1 h to obtain the epoxy/TiO_2 hybrid solution. The various compositions used to synthesize epoxy/TiO_2 hybrid materials are shown in Table 1. The solution was spin-coated on silicon wafer and glass for 20 s at a speed of 2000 rpm. The coated films were cured on a hot plate at 50 °C for 1 h, 80 °C for 2 h, and 120 °C for 12 h to obtain the epoxy/TiO_2 hybrid films.

2.4. Characterization

Fourier transform infrared (FTIR) spectra of the prepared thin films were obtained on double-polished silicon wafers by using a Perkin Elmer Spectrum spectrophotomer. With the rated power 4 kW, horizontal goniometer with 185 mm radius, continuous scanning mode with 0.03° interval and 1.0 s counting time, the X-ray powder diffraction data were collected at room temperature on the X-ray diffractometer (XRD) (Philips Corp., The Netherlands) using Cu K_α radiation, $\lambda = 1.54056$ Å between 20° and 60° (2θ). The operation voltage and anode current were 40 kV and 30 mA, respectively. Thermogravimetric analysis (TGA) and differential scanning calorimetry (DSC) were performed under a nitrogen flow using a DuPont Model 951 for thermogravimetric analysis and a DuPont Model 910S differential scanning calorimeter at a heating rate of 20 °C/min and 10 °C/min, respectively. The TGA and DSC samples were prepared by spin-coating the precursor solution on a glass substrate, followed by curing at various temperatures, as described in Section 2.3. The transmittance of the prepared films was measured using an ultraviolet–visible (UV–vis) spectrophotometer (Jasco V-570). An ellipsometer (GES-5E SOPRA) was used to measure the refractive index and the extinction coefficient of the prepared films in the wavelength range of 190–900 nm. The thickness (h) of the prepared films was determined simultaneously. An atomic force microscopy (AFM) (Digital Instrument, Inc., Model DI 5000 AFM) with a monolithic silicon probe was used to assess the surface morphology of the coated films under the tapping mode. The shape of the probe tip was similar to a polygon-based pyramid, and the height ranged between 10 and 15 μm. The baseline noise was less than 0.1 nm. The fracture surfaces of hybrid thin films were examined on a Hitachi H-2400 Scanning Electron Microscope (FE-SEM) at a voltage of 10 kV.

Table 1
Monomer compositions (wt.%) for preparing the hybrid thin films.

Sample (no.)	DGEBA	IPTES	TiO_2	MHHPA
METi0	67	7	0	27
METi2	65	7	2	26
METi4	64	6	4	26
METi10	60	6	10	24
METi15	57	6	15	23
METi25	50	5	25	20
METi35	43	5	35	17
METi50	33	3	50	13

DGEBA:IPTES:MHHPA = 1:0.1:0.8 (mole ratio).

3. Results and discussion

3.1. Analysis of chemical structure

Fig. 2 shows the FTIR spectra of (a) IPTES/epoxy mixture, (b) IPTES/epoxy mixture reacted for 3 h, (c) epoxy/TiO_2 hybrid material before curing, and (d) epoxy/TiO_2 hybrid material after curing. The absorption band in spectrum (a) at 3400 and 916 cm^{-1} was assigned to the OH and epoxy group from DGEBA. The absorption band at 2271 cm^{-1} was assigned to the –N═C═O group from a coupling agent. As shown in spectrum (b), the intensity of absorption peaks at 3400 and 2271 cm^{-1} decreased after reacting for 3 h, indicating that the reaction occurs between the epoxy resin and coupling agent. Moreover, the absorption band at 3400 cm^{-1} becomes obvious again because of the OH group on the TiO_2 particles. After curing, the absorption peaks of the epoxy resin and OH group disappeared. In addition, the absorption band of Ti–O–Si appeared at 1100 cm^{-1}, and that of Ti–O–Ti appeared at 600 cm^{-1}. The result indicates that the epoxy/TiO_2 hybrid materials with desired chemical structure were prepared.

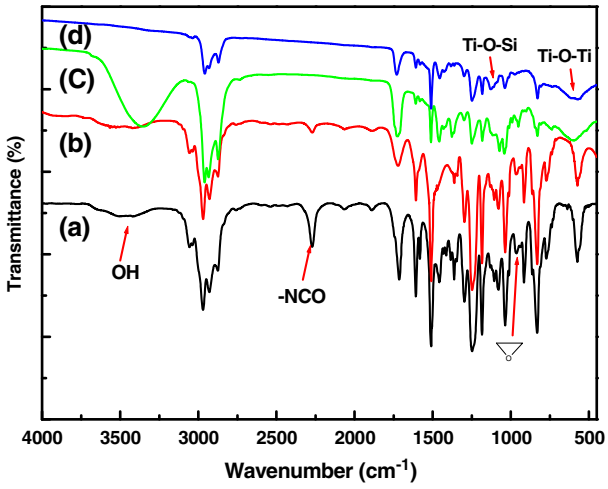

Fig. 2. FTIR spectra of (a) IPTES/epoxy mixture, (b) IPTES/epoxy mixture reacted for 3 h, (c) hybrid material before curing, and (d) hybrid material after curing.

Table 2
The thermal, surface, and optical properties of hybrid materials.

Sample	Td (°C, 95 wt.%)	Residue[a] (wt.%, 800 °C)	Thickness (um)	Ra[b] (nm)	Ra/h (%)	Rq[b] (nm)	Rq/h (%)	n_{633}[c] (nm)	k_{633}[c]	Vd[d]
METi0	289.8	17.29	0.970	0.219	0.23	0.274	0.282	1.450	6.83×10^{-3}	14.43
METi2	218.4	21.36	0.870	0.273	0.31	0.321	0.370	1.493	5.77×10^{-3}	27.66
METi4	225.6	24.38	0.627	0.293	0.62	0.365	0.773	1.557	3.27×10^{-3}	30.25
METi10	233.1	25.50	0.472	0.296	0.61	0.368	0.779	1.593	1.68×10^{-3}	38.93
METi15	220.0	33.85	0.480	0.298	0.62	0.373	0.819	1.596	1.08×10^{-3}	41.93
METi25	216.5	42.15	0.424	0.332	0.78	0.416	0.981	1.587	1.39×10^{-3}	32.78
METi35	227.3	47.31	0.296	0.306	1.03	0.384	1.29	1.636	6.65×10^{-3}	24.65
METi50	221.1	56.23	0.281	0.751	2.67	0.947	3.37	1.639	5.13×10^{-3}	22.27

[a] Experimental results from TGA values based on the assumption that only inorganic moieties are present at 900 °C.
[b] Ra and Rq are the average and root mean square roughness, respectively.
[c] n and k are the refractive index and extinction coefficient at 633 nm, respectively.
[d] Vd is the Abbe number.

3.2. Thermal properties

The DSC curves of epoxy/TiO_2 hybrid materials (METi0–METi10) obtained from various TiO_2 solid contents show that the IPTES/epoxy material has a thermal glass (T_g) point at 80 °C. Tg increased to 115 °C as 2 wt.% of TiO_2 was added into the epoxy matrix. No obvious T_g point was observed when the TiO_2 content was larger than 10 wt.%. The result might be caused by the formation of epoxy resin network that is strongly restricted by the hybridization within the TiO_2 network [20]. The heat resistance of cured epoxy resin improved considerably with increased TiO_2 content. On the other hand, the TGA curves of the hybrid materials (METi0–METi50) show that all hybrid samples exhibited slight weight loss at the beginning because of the volatilization of the moisture or solvent. The obvious weight loss was observed in the range of 150–300 °C, indicating a certain degree of degradation for the polymer, a small amount of hydrolysis condensation of the unfinished OH functional groups, and the production of an oligomer. The second weight loss from 300 °C to 600 °C corresponded to the decomposition of the organic component. The weight loss decreased as the TiO_2 content increased. The result showed that the TiO_2-modified epoxy resin formed the network structure. The thermal decomposition (T_d) point and residue of the hybrid material are shown in Table 2.

3.3. Microstructure analysis

The surface morphology and roughness of the prepared hybrid coatings was analyzed using AFM and FE-SEM images. The AFM and FE-SEM images of the prepared epoxy/TiO_2 hybrid materials showed that no defects and phase separation were observed, and that the surface roughness of the hybrid coatings was low. The average roughness (Ra) and mean square roughness (Rq) of the coatings are shown in Table 2. It shows that the surface roughness increases with the TiO_2 content. The values of R_a and R_q increased from 0.219 and 0.274 nm for 0 wt.% TiO_2 to 0.751 and 0.947 nm for 50 wt.% TiO_2, respectively. However, under various operational conditions, all ratios of roughness and thickness were below 3.4%. This result indicates the excellent planarity of the prepared hybrid films. The lower surface roughness reduced the optical loss, which further confirms the feasibility of applying hybrid materials to thin films. It is known that if the aggregation of TiO_2 nanoparticles occurred, the phase separation would be observed, especially when TiO_2 content was high. However, we cannot found any phase separation from the images of FE-SEM and AFM. Therefore, the phase separation caused by blending of TiO_2 could be negative in the present study. Fig. 3 shows the XRD patterns of the epoxy/TiO_2 hybrid materials with various TiO_2 solid contents. A broad peak was observed at approximately 20° because of the amorphous nature of the epoxy resin [2]. The XRD patterns of the hybrid material revealed dominant peak with values of 2θ located at 25.3°, 27.9°, 47.8°, and 54.1°, corresponding to the (101), (004), (200), and (105) planes, respectively. It indicates that the embedded TiO_2 has the crystal phase of anatase. However, the peak intensity of TiO_2 is not obvious as the TiO_2 content is about 10–35 wt.%. As the TiO_2 content is higher than 50 wt.%, the peaks of anatase TiO_2 can be observed clearly. This result is corresponding to the experimental design.

3.4. Optical properties

Fig. 4(a) and (b) shows the optical transmission spectra of the hybrid coatings prepared from various TiO_2 solid contents and curing temperatures, respectively. The figures show that the transmittances of the hybrid films are high in the visible range and slightly decrease with increasing TiO_2 content and curing temperature. This occurs because the surface roughness of the hybrid film gradually increased; thus, the light through the film was subject to interference or an interference phenomenon. However, all hybrid films exhibited excellent transmittance of more than 95% in visible light. Fig. 5 shows L.a.b. color analysis of (a)–(c) METi0 and (d)–(f) METi10 after thermal treatment for 6 h at curing temperatures of 80 °C, 120 °C, and 150 °C. The detailed data of luminance, transmittance, and the decay rate of the prepared epoxy/TiO_2 hybrid materials are shown in Table 3. It shows that the transparency and luminance of hybrid thin films decrease with increasing curing temperature and TiO_2 content. At a high TiO_2 content, the influence of curing temperature on the transparency and luminance of hybrid thin films becomes obvious. The values of the decay rate for luminance decay rate (D_L)

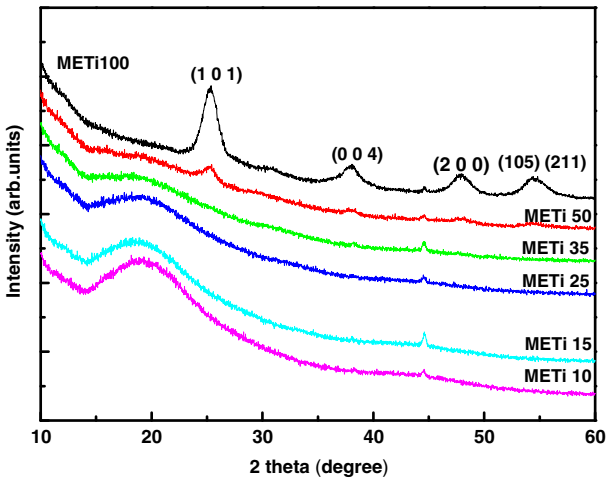

Fig. 3. XRD patterns of epoxy/TiO_2 hybrid materials, METi10–METi100.

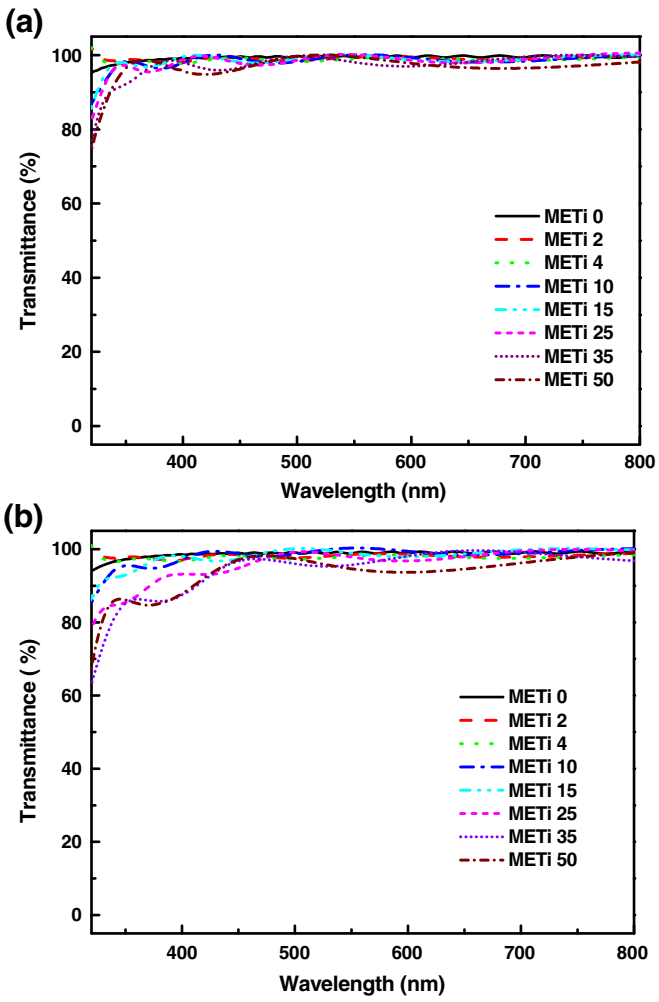

Fig. 4. Transmittance UV–vis spectra of epoxy/TiO_2 hybrid films cured at (a) 80 °C and (b) 150 °C, respectively.

and transmittance decay rate (D_T) at a fixed curing temperature of 150 °C were 0.29 and 1.06 for 10 wt.% TiO_2 content. However, the values of D_L and D_T increased to 2.04 and 4.96 as the TiO_2 content increased to 50 wt.%. Under various operational conditions, no yellowing of the hybrid films was observed, and the average transmittance and luminance was over 90% and 97%, respectively. On the other hand, the ultraviolet lamp (365 nm) exposure test of hybrid films at exposure times of 4 h shows that no yellowing was observed. This result indicates the excellent optical properties of the prepared hybrid films. The detailed experimental data are shown in Table 4. As displayed in the table, the exposure time has no evident influence on the luminance and transmittance of hybrid films because the TiO_2 content is fixed. This result also indicates excellent optical properties of the prepared hybrid films. The values of refractive index and extinction coefficient of hybrid films measured from ellipsometer analysis were listed in Table 2. It shows that the refractive index (at a wavelength of 633 nm) increased from 1.450 to 1.639 as the *TiO_2 content increased from 0 to 50 wt.%*. This occurred because TiO_2 has a higher refractive index than epoxy. This result suggests that the n of the prepared hybrid films is tunable through the TiO_2 content. The extinction coefficient of the hybrid films was almost zero, indicating that the prepared hybrid coating has excellent optical transparency in the visible region.

Table 3
Luminance and transmittance of epoxy/TiO_2 hybrid materials obtained at different TiO_2 contents and curing temperatures.

	Temp. (°C)	L[a] (%)	D_L (%)[b]	T%[c] (400 nm)	$D_{T400\ nm}$[d] (%)	T% (550 nm)	$D_{T550\ nm}$ (%)
METi0	80	99.87	–	99.47	–	99.56	–
	120	99.80	0.07	99.27	0.20	99.40	0.16
	150	99.52	0.35	98.53	0.95	98.84	0.73
METi10	80	99.71	–	99.58	–	99.98	–
	120	99.51	0.20	99.22	0.36	99.32	0.65
	150	99.42	0.29	98.04	1.54	98.92	1.06
METi15	80	99.66	–	98.79	–	99.95	–
	120	99.34	0.32	97.81	0.99	99.14	0.8
	150	98.88	0.87	93.16	5.70	97.85	2.10
METi35	80	99.04	–	98.08	–	98.08	–
	120	98.37	0.68	92.01	6.18	95.90	2.22
	150	98.26	0.79	87.48	10.80	95.68	2.45
METi50	80	99.46	–	95.83	–	99.55	–
	120	98.47	0.99	91.04	5.00	97.01	2.55
	150	97.43	2.04	87.81	9.35	94.61	4.96

[a] L: luminance.
[b] D_L: luminance decay rate = $(L_T - L_{80\ °C} / L_{80\ °C}) * 100\%$.
[c] T%: transmittance (%).
[d] D_T: transmittance decay rate = $(T_T - T_{80\ °C} / T_{80\ °C}) * 100\%$.

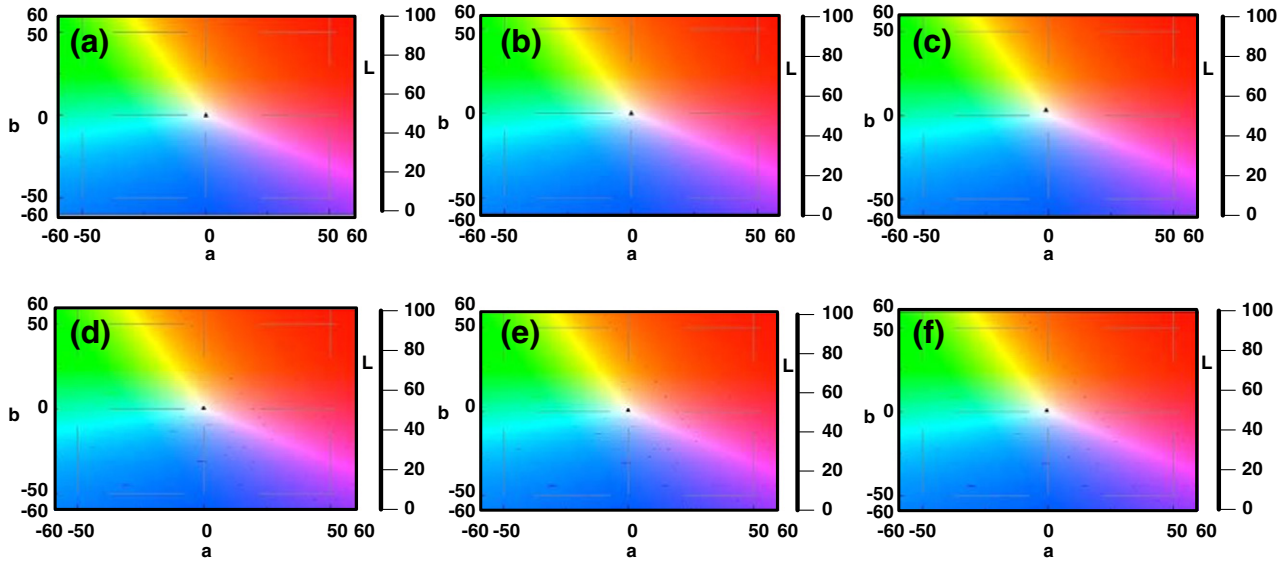

Fig. 5. L.a.b. color analysis of (a)–(c) METi0 and (d)–(f) METi10 after curing for 6 h at different temperatures, 80 °C, 120 °C, and 150 °C, respectively.

Table 4
Luminance and transmittance of epoxy/TiO_2 hybrid materials obtained at different TiO_2 contents and ultraviolet lamp exposure times, 0–4 h.

	Time (h)	L[a] (%)	D_L[b] (%)	T%[c] (400 nm)	$D_{T400\ nm}$[d] (%)	T% (550 nm)	$D_{T550\ nm}$ (%)
METi0	0	99.52	–	98.80	–	99.00	–
	0.5	99.46	0.06	98.49	0.34	98.81	0.19
	1	99.46	0.06	98.46	0.34	98.75	0.25
	2	99.33	0.19	98.45	0.34	98.61	0.39
	4	99.28	0.24	98.36	0.44	98.59	0.41
METi15	0	99.23	–	98.09	–	98.99	–
	0.5	99.22	0.01	97.77	0.32	98.68	0.34
	1	99.18	0.05	97.76	0.33	98.48	0.54
	2	99.14	0.09	97.64	0.46	98.36	0.64
	4	99.07	0.16	97.57	0.53	98.34	0.66
METi25	0	99.18	–	96.37	–	99.09	–
	0.5	98.88	0.30	95.68	0.71	98.53	0.56
	1	98.50	0.68	95.59	0.81	98.46	0.64
	2	98.37	0.82	95.59	0.81	98.38	0.72
	4	98.35	0.83	95.49	0.94	98.37	0.73
METi35	0	98.80	–	93.06	–	96.68	–
	0.5	98.59	0.21	93.05	0.01	96.65	0.03
	1	98.57	0.23	03.02	0.04	96.65	0.03
	2	98.44	0.36	92.87	0.20	96.38	0.31
	4	98.36	0.45	92.83	0.25	96.36	0.33
METi50	0	98.74	–	90.74	–	98.01	–
	0.5	98.61	0.13	90.64	0.11	97.73	0.27
	1	98.59	0.15	90.33	0.45	97.51	0.51
	2	98.56	0.18	90.21	0.58	97.45	0.57
	4	98.52	0.22	90.12	0.68	97.35	0.67

[a] L: luminance.
[b] D_L: luminance decay rate $= (L_T - L_{80\ °C} / L_{80\ °C}) * 100\%$.
[c] T%: transmittance (%).
[d] D_T: transmittance decay rate $= (T_T - T_{80\ °C} / T_{80\ °C}) * 100\%$.

Conversely, the Abbe number of the prepared hybrid films increased to a maximal value of 41.93 as the TiO_2 content increased from 0 to 20 wt.%. The Abbe number subsequently decreased to 22.27 as the TiO_2 content increased to 50 wt.%. In physics and optics, the Abbe number is a measure of the dispersion of material; high values of the Abbe number indicate low chromatic aberration. Generally, a typical Abbe number value is approximately 30 for hybrid films used in optical applications. It is known that the polyamide and aliphatic amine is extensively used as curing agents for preparing epoxy resin. However, the prepared epoxy yellows after cured when exposed to moisture or excessive heat. In the present study, 4-methylhexahydrophthalic anhydride and n,n-dimethylbenzylamine were used as the curing agent and accelerator, respectively, which could combine with the hybridization of titania to prevent the yellowing phenomena of epoxy resin. Incorporation of titania nanoparticles into the epoxy matrix not only increases the refractive index of hybrid materials but also improves the yellowing resistance. The L.a.b. analysis also confirmed that no yellowing phenomena of TiO_2/epoxy films were observed in this study.

3.5. Water-absorbing test

Water absorption data were obtained by immersion in water for one week at 60 °C. After removal, the specimens were dried and weighed immediately. The increase in weight is reported as a percentage. Various materials absorb varying amounts of water, and the presence of absorbed water may affect materials in various manners. Optical, electrical, and optoelectronic properties change noticeably with water absorption; therefore, materials that absorb almost no water are favorable for these applications. Table 5 shows the water absorption test for the METi0–METi50 hybrid materials.

Table 5
Water absorbing test for the epoxy/TiO_2 hybrid materials.

Sample	Before W_{dry} (g)	After W_{wet} (g)	A_W[a] (%)
METi0	1.8365	1.8375	0.05
METi15	1.7862	1.7865	0.02
METi25	1.6554	1.6574	0.12
METi35	1.8140	1.8143	0.02
METi50	1.7050	1.1054	0.02

[a] A_w: water absorbing rate $= (W_{wet} - W_{dry} / W_{dry}) * 100\%$.

As shown in Table 5, the low water absorption rate of the prepared epoxy/TiO_2 hybrid materials has a negligible effect on their properties, especially when used under a high-humidity environment.

4. Conclusion

Epoxy/TiO_2 hybrid materials were prepared using the sol–gel method. DSC analysis indicated that the T_g and thermal stability of the hybrid materials increased with TiO_2 content. The TGA indicated that all prepared hybrid materials had an excellent T_d above 200 °C. The *FE-SEM and* AFM images showed that the hybrid material had an excellent film-forming property and surface planarity. *XRD analysis showed that the titania in the hybrid material had a crystal phase of anatase.* The ellipsometer analysis in n and k and UV–vis measurement showed that the transparency of hybrid thin films was above 90%, and that L.a.b. color analysis indicated that luminance was above 95%; no yellowing was observed. Furthermore, the value of the refractive index (at a wavelength of 633 nm) increased from 1.450 to 1.638 as the *TiO_2 content increased from 0 to 50 wt.%.* Under an ultraviolet environment, the transparency of the hybrid material was above 90%, and no yellowing was observed. In addition, the hybrid materials exhibited a low hydroscopic property under a high-humidity environment.

Acknowledgments

The authors would like to acknowledge the financial support of the National Science Council through project NSC 101-2221-E-131-006-MY3.

References

[1] M. Ochi, D. Nii, Y. Suzuki, M. Harada, J. Mater. Sci. 45 (2010) 2655.
[2] K.H. Ding, G.L. Wang, M. Zhang, Mater. Des. 32 (2011) 3986.
[3] K. Shikinaka, K. Aizawa, Y. Murakami, Y. Osada, M. Tokita, J. Watanabe, K. Shigehara, J. Colloid Interf. Sci. 369 (2012) 470.
[4] K. Luo, S. Zhou, L. Wu, Thin Solid Films 517 (2009) 5974.
[5] Y.Y. Yu, W.C. Chien, S.Y. Chen, Materials and Design 31 (2010) 2061.
[6] W. Jianye, L.W. Garth, Chem. Mater. 8 (1996) 1667.
[7] Y. Chujo, E. Ihara, S. Kure, K. Suzuki, T. Saegusa, Makromol. Chem. Macromol. Symp. 42 (1991) 303.
[8] L. Mascia, A. Kioul, Polymer 36 (1995) 3649.
[9] M.A. Harmer, W.E. Farneth, Q. Sun, J. Am. Chem. Soc. 118 (1996) 7708.
[10] R. Tamki, K. Naka, Y. Chujo, Polym. Bull. 39 (1997) 303.
[11] Y. Imai, N. Yoshida, Y. Chujo, Polym. J. 310 (1999) 258.
[12] B. Munro, P. Conrad, S. Kramer, H. Schmidt, Sol. Energy Mater. Sol. Cells 54 (1998) 131.
[13] C. Sanchez, F. Ribot, B. Lebeau, J. Mater. Chem. 9 (1999) 35.
[14] Y.Q. Rao, B. Antalek, J. Minter. Langmuir 25 (2009) 12713.
[15] B.T. Liu, S.J. Tanga, Y.Y. Yu, S.H. Lin, Colloids Surf. A Physicochem. Eng. Asp. 377 (2011) 138.
[16] F. Bauer, U. Decker, H. Ernst, M. Findeisenb, H. Langguth, R. Mehnert, V. Sauerland, R. Hinterwaldner, Int. J. Adhes. Adhes. 26 (2006) 567.
[17] J.L.H. Chau, C.T. Tung, Y.M. Lin, A.K. Li, Mater. Lett. 62 (2008) 3416.
[18] J.L.H. Chau, H.W. Liu, W.F. Su, J. Phys. Chem. Solids 70 (2009) 1385.
[19] L. Sowntharya, S. Lavanya, G. Ravi Chandra, N.Y. Hebalkar, R. Subasri, Ceramics Int. 38 (2012) 4221.
[20] Y. Liu, C. Lu, M. Li, L. Zhang, B. Yang, Colloids Surf. A Physicochem. Eng. Asp. 328 (2008) 67.